



Application of Taguchi experimental design methodology in optimization for adsorption of phosphorus onto Al/Ca-impregnated granular clay material

Yang Yu^a, Nan Chen^{a,b,*}, Weiwu Hu^c, Chuanping Feng^{a,b}

^aSchool of Water Resources and Environment, China University of Geosciences (Beijing), Beijing 100083, China, Tel. +86 18010033186; email: yuyang1914@gmail.com (Y. Yu), Tel. +86 10 82322281; Fax: +86 10 82321081; email: cnjing2008@hotmail.com (N. Chen), Tel. +86 13801205306; email: fengchuanping@gmail.com (C. Feng)

^bKey Laboratory of Groundwater Cycle and Environment Evolution, Ministry of Education (China University of Geosciences (Beijing)), Beijing 100083, China

^cThe Journal Center, China University of Geosciences (Beijing), Beijing 100083, China, Tel. +86 13811783404; email: huzweiwu010@163.com (W. Hu)

Received 15 March 2014; Accepted 3 September 2014

ABSTRACT

The adsorption of phosphorus in a fixed bed was investigated using the Taguchi experimental design. The abilities of two types of granular adsorbents, Al- and Ca-impregnated granular clay materials (Al-GCM and Ca-GCM), to adsorb phosphorus from an aqueous solution were evaluated, then controllable factors (the adsorbent material, initial phosphorus concentration, and flow rate) were optimized. An L_9 orthogonal array was used for the experimental design, and the conditions were optimized to achieve the best signal-to-noise ratio. The optimal conditions were using Ca-GCM as the material, an initial phosphorus concentration of 20 mg/L, and a flow rate of 600 μ L/min. Under these conditions, the number of bed volumes at the breakthrough point was 354 and the Ca-GCM adsorption capacity for phosphorus was 9.12 mg/g. The relative importance of each controllable factor was determined using the analysis of variance method, which revealed that the type of adsorbent was the most influential factor, accounting for 55.5% of the phosphorus removal capacity. The initial phosphorus concentration was the next most influential factor, contributing 35.7% of the phosphorus removal capacity. The flow rate contributed only 8.8% of the phosphorus removal capacity. The main component of the product of the adsorption process was hydroxylapatite, which could be used in many industrial and agricultural processes. The treatment process was found to be relatively environmentally benign, and would be a way of regenerating phosphorus without causing secondary pollution.

Keywords: Taguchi design; Al- and Ca-impregnated clay material; Phosphorus adsorption; Recycling

1. Introduction

Phosphorus is widely used in agriculture and in industrial processes, and some phosphorus is often

transferred from where it is used to freshwater ecosystems because of rainwater runoff [1]. Phosphorus contributes to the eutrophication of aquatic ecosystems, which is currently one of the most important problems in reservoirs, rivers, lakes, and coastal waters [2,3]. Increasing concern about the effects of eutrophication

*Corresponding author.

has led to more stringent environmental regulations being implemented in recent years [4]. Phosphorus is considered to be a key limiting nutrient for algae in natural water bodies, so there is a growing demand for methods to remove phosphorus from water [5]. Increasing demand for phosphorus for use in the agricultural and industrial sectors and the gradual exhaustion of phosphate ore deposits have resulted in the recycling of phosphorus becoming important.

Conventional treatments for removing phosphorus from water include physical [6], chemical [7,8], and biological [9] methods. Physical treatments, such as electro dialysis and ion exchange, are costly and inefficient. Chemical treatments, such as precipitation with Al, Ca, or Fe, are suitable for treating water that contains high phosphorus concentrations, but are less effective for treating water that contains low phosphorus concentrations. The disposal of the sludge produced by the precipitation of phosphorus, and neutralization of the effluent, are problematic. Biological treatments, such as treatment with activated sludge, can offer certain advantages over the chemical precipitation method, because biological treatments do not require the addition of large amounts of chemicals. However, biological treatments can be very sensitive to the concentrations of organic chemicals and the temperature [3]. Adsorption is widely used to remove phosphorus from water because it offers a high removal efficiency and because it is relatively simple and inexpensive to use this method [10,11]. The adsorption method also enables the phosphorus removed from the water to be recycled because the phosphorus can be removed from the product and used in a number of agricultural or industrial processes. However, a large amount of spent liquor is produced during the recycling process [12]. A wide range of adsorbents, such as steel slag [11,13], active carbon [14], fly ash [15], goethite [16], biochar [17], and shells [18], have been used to remove phosphorus from water. In a previous study, we prepared two composite clay materials, an Al-impregnated granular clay material (Al-GCM) and a Ca-impregnated granular clay material (Ca-GCM), and we performed batch experiments to determine the effects of the initial phosphorus concentration, contact time, and initial pH on the ability of these materials to remove phosphorus from water [19,20]. When a phosphorus removal system is used in practice, a fixed bed adsorption system can make full use of the adsorbent and be easily reused, but it is difficult to apply the results of batch tests to a fixed bed system. Therefore, it is necessary to comprehensively study a fixed bed adsorption system to optimize the operating parameters.

The Taguchi method is a statistical experimental design that is widely used to design a process and to improve the quality of the product [19]. Many applications of the Taguchi method have been reported. For example, Engin et al. used the Taguchi method to optimize the process conditions (such as the feed flow rate, bed height, and dye concentration) for removing dye from water [20]. İrdemez et al. used the Taguchi method to determine the optimum conditions for removing phosphate from water by electrocoagulation [21]. However, the Taguchi method has rarely been used to optimize a fixed bed system for adsorbing phosphorus from water.

In the study presented here, breakthrough tests were performed to assess the performances of a fixed bed system under different conditions. Specifically, the phosphorus uptake by the Al-GCM and Ca-GCM adsorbent filters as a function of the flow rate and the phosphorus concentration in the inflow solution were investigated using the Taguchi experimental design method. The optimum combination of parameters for the fixed bed adsorption system was then determined, and the relative importance of each parameter was confirmed using the analysis of variance (ANOVA) method. The degree to which each parameter influenced the phosphorus removal efficiency was determined and will be important in later experiments. The ability to recycle phosphorus using the system was tested using a physical method after the breakthrough study had been performed.

2. Materials and methods

2.1. Experimental materials and setup

All of the reagents used in this study were of analytical grade. A 1,000 mg/L phosphorus stock solution was prepared by dissolving 7.7480 g of NaH_2PO_4 (Sinopharm Chemical Reagent Co., Ltd, China) in deionized water. Solutions containing different phosphorus concentrations were prepared for use in the column tests by diluting the stock solution with deionized water.

Dolomite and montmorillonite were supplied by Zhenyongwei Technology Development Co., Ltd (Beijing, China). Scallop shells (used as a calcium source) were collected from a local restaurant in Beijing, China, and they were ground to a powder. The dolomite, montmorillonite, and scallop shell powders had particle sizes of <120 , <100 , and <200 μm , respectively. The Al-GCM adsorbent was prepared by mixing dolomite, montmorillonite, soluble starch, and $\text{Al}_2(\text{SO}_4)_3$ at a ratio of 3:3:2:2 (by mass). The Ca-GCM adsorbent was prepared by mixing scallop shell powder, montmorillonite, and soluble starch at a ratio of

1:1:1 (by mass). The two types of adsorbent were each manually formed into spherical samples after ultra-pure water had been added. The adsorbent granules were then dried in an oven (Tianjin Tec 101-2ab, China) at 105°C and then calcined in a muffle furnace (Nabertherm P330, Germany) at 600°C. The preparation of the granular adsorbent impregnated with a mixture of Al and Ca is described elsewhere [22,23].

A schematic diagram of the column adsorption system is shown in Fig. 1. Adsorbent granules were packed into nine plexiglass columns (each with an inner diameter of 30 mm and a length of 200 mm). The effective height of the adsorbent-packed section in each column was 100 mm. The working volume of each column was 43.6 mL and the pore volume was 22.68 mL. Three peristaltic pumps (Longer BT100-1F, China) were used to pump water upwards through the nine fixed columns, and samples of the effluents were collected from the top of each column at regular intervals. Each test was performed in triplicate, and every data point in the breakthrough study is the mean of those triplicate tests.

2.2. Experimental procedure

Studies using Taguchi's orthogonal arrays are highly efficient compared with full factorial experiments [24]. For example, 1,024 experiments would have to be conducted to investigate five factors at four levels using a full factorial experiment, but only 16 experiments would be needed using Taguchi's orthogonal method. Each row in the orthogonal array indicates one run with a unique set of values for the different parameters [25,26].

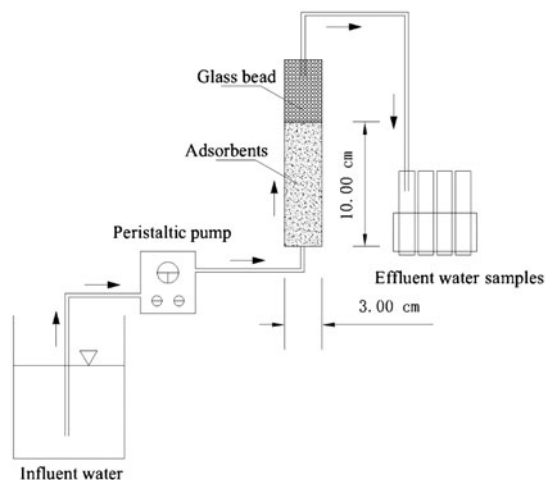


Fig. 1. Schematic diagram of lab-scale column study (a column volume of 141 mL; a dry mass of 33 g).

Range analysis using the average response value is usually performed to determine the optimal combination of process parameters. The ANOVA method is used to determine which factors are statistically significant [27].

In this study, the Taguchi experimental design (L_9 orthogonal array) was used to identify the optimal conditions and the most appropriate adsorbent for use in the column adsorption process to remove phosphorus from water. The controllable factors included the adsorbent material, inflow rate, and initial phosphorus concentration. The values for each of these factors were determined from the results of previous investigations [22,23] and are given in Table 1. The same phosphorus concentration was used in this study as in the batch study that we performed previously so that the results of this study could be compared with the results of the previous study. Besides flow rate and phosphorus concentration were determined at a suitable extent to ensure result is noteworthy and avoid taking too long time. The values of the specific factors that were used for each column test are shown in Table 2. The empty bed contact times at flow rates of 600, 800, and 1,000 $\mu\text{L}/\text{min}$ were 1.21, 0.91, and 0.73 h, respectively. The adsorption performance of a selected bed was evaluated at the maximum bed volume (BV) at the breakthrough point ($C_t/C_0 = 0.05$). A breakthrough curve was constructed by plotting the normalized effluent phosphorus intensity (C_t/C_0) against the operation time or the BV. The BV was calculated using the following equation [28].

$$BV = V_F/V_R \quad (1)$$

The saturation capacity of the adsorbent in the fixed bed system was calculated using the following equation [29]:

$$q_e = \int_0^{V_F} (C_0 - C_t) dV_F/m \quad (2)$$

where V_F is the total water volume flowing through the selected column (mL), V_R is the pore volume of the adsorption column (mL), C_0 is the influent phosphorus concentration (mg/L), C_t is the effluent phosphorus concentration (mg/L), q_e is the amount of phosphate adsorbed on the adsorbent (mg/g), and m is the mass of the adsorbent (g).

After the adsorption tests were complete the adsorbents were tested for the possibility of the phosphorus being recycled. Each used adsorbent samples was dried in an oven at 105°C. The white powder adhering to each adsorbent fell off spontaneously during the

Table 1
Factors and levels for the Taguchi L_9 optimization experiment

Process parameter	Designation	Level 1	Level 2	Level 3
Flow rate ($\mu\text{L}/\text{min}$)	A	600	800	1,000
P concentration (mg/L)	B	20	30	40
Adsorbent material	C	Ca-GCM	Al-GCM	Ca/Al-GCM

Table 2
Chemical analysis of each adsorbent by SEM–EDS test

Composition (wt%)	C	O	Mg	Al	Si	S	Ca	P
Pristine Al-GCM	2.95	44.60	6.86	7.47	13.71	9.90	4.89	–
Used Al-GCM	2.75	54.35	3.01	6.51	11.92	8.50	3.81	9.16
Pristine Ca-GCM	7.35	55.27	1.90	3.56	9.49	1.86	25.56	–
Used Ca-GCM	7.78	58.16	0.36	2.66	8.68	–	20.95	10.41

drying process and collected in the bottom of the glass container. The composition of white powder was determined by X-ray diffraction (XRD) analysis (D8 FOCUS; Bruker, Germany).

2.3. Analytical methods

The phosphorus concentration in each aqueous sample was measured using the ammonium molybdate spectrophotometric method, with detection at 700 nm (Hach DR/5000, USA). Each aqueous sample was filtered through a 0.45 μm cellulose filter to remove small colloids before the analysis was performed. The effluent from each column was collected every 6 h, at which time the pH of the solution was determined using a standard pH meter (Orion 8157BNUMD, USA) and the aluminum concentration was measured by inductively coupled plasma mass spectrometry (using a 7500C instrument; Agilent Technologies Inc., USA). The morphological features of each adsorbent were determined and spot elemental analyses of the adsorbents were performed using scanning electron microscopy (SEM) coupled with energy dispersive X-ray spectroscopy (EDS) (SSX-550; Shimadzu Corp., Japan). The mineral composition of white powder was determined by XRD (Bruker D8 FOCUS).

3. Results and discussion

3.1. Characterization of the adsorbents

An SEM image was taken of the Ca-GCM before and after it had been used in an adsorption test, and the images are shown in Fig. 2(A) and (B). It can be

seen that the Ca-GCM had a loose and coarse surface morphology before it had been used to adsorb phosphorus, and this was caused by the soluble starch being burned off during the calcining process. We predicted that this porous structure would have a positive effect on the phosphorus adsorption process. There were abundant agglomerates of globular particles still adhering to the surface of the adsorbent after it had been used in an adsorption test. Manually measuring micropores leads to unacceptable errors and poor precision, and is an inefficient process. Therefore, the “Pores (Particles) and Cracks Analysis System” (PCAS), which can accurately compute various geometric parameters, has been developed to quantify microstructures [30]. We used the PCAS to analyze the SEM images of Ca-GCM before and after it had been used to adsorb phosphorus, to determine how the microstructure changed during the adsorption process. As expected, the porosity decreased from 40.57 to 26.04% (Fig. 2(C) and (D)). CaO can easily and instantly be dissolved to form Ca^{2+} and OH^- in an aqueous solution. The pH of the effluent was 8.2 because of the hydrolysis of CaO in the adsorbent. It has been shown that the dominant orthophosphate species is phosphate at pH values above 7, dihydrogen phosphate at pH 3–7, and hydrogen phosphate at pH values less than 3. At the pH values of the test effluents, therefore, phosphate will combine with calcium ions to form a precipitate that will adhere to the surface of the adsorbent. It is therefore possible that the mechanism by which Ca-GCM adsorbs phosphorus is actually a chemical precipitation process. This process can be described in a simple way using the following equations [22].

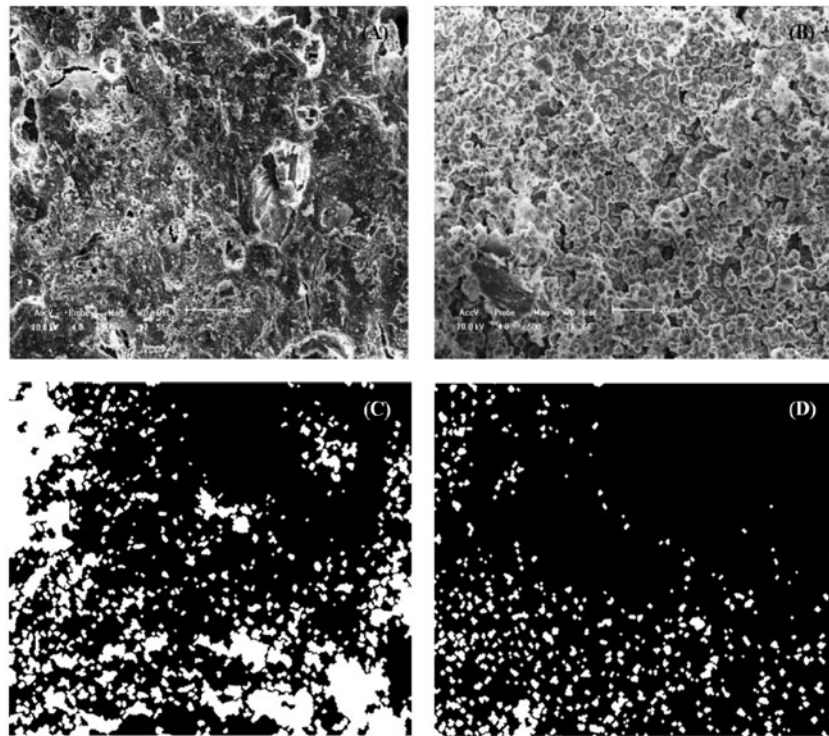
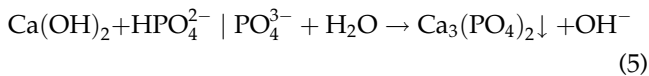
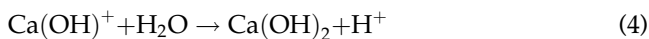
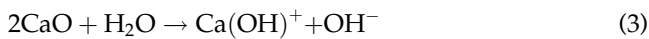
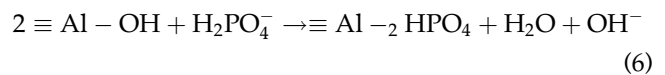


Fig. 2. SEM images of (A) the pristine Ca-GCM; (B) the used Ca-GCM from the adsorption column; (C) the binary diagrams of the pristine Ca-GCM; and (D) the used Ca-GCM from the adsorption column calculated by PCAS.



adsorption mechanism involved is a complex mix of ligand exchange and chemical precipitation processes [23,32]. The adsorption process that is assumed to occur is represented in the following equation.



Ligand exchange and electrostatic attraction may play secondary roles in the removal of phosphorus by the adsorbents [31].

The unused Al-GCM had a similar porous surface construction to that of the unused Ca-GCM (Fig. 3(A)) because they were produced using a similar process. However, the Al-GCM that had been used to adsorb phosphorus had a clearly different morphology from that of the used Ca-GCM. Specifically, the surface of the used Al-GCM was covered with abundant schistose sedimentation (Fig. 3(B)), and the PCAS showed that the porosity of the Al-GCM dropped from 36.38 to 12.31% during the adsorption process. Both the SEM images and the binary images that were obtained (Fig. 3(C) and (D)) indicated that phosphorus was adsorbed onto the surface of the Al-GCM. Al_2O_3 has been found to adsorb phosphate effectively, and the

The pH of the effluent from the Al-GCM was 8.4 because OH^- was generated in the adsorption process. It has been reported that, aluminum ions exist in the form $\text{Al}(\text{OH})_4^-$ when the pH is higher than 8. Both phosphate and $\text{Al}(\text{OH})_4^-$ will be negatively charged at the effluent pH, so the efficiency at which phosphate can be coagulated will be relatively low, meaning that it is possible that ligand exchange and surface precipitation will be involved in the adsorption of phosphorus by the Al-GCM.

The components in the Al/Ca-GCM after it had been used for the adsorption process were identified by EDS, and the results are presented in Table 2. Our previous studies showed that aluminum and calcium were the effective constituents in the adsorbents, and the presence of phosphorus was taken as evidence that surface adsorption reactions occurred. Aluminum

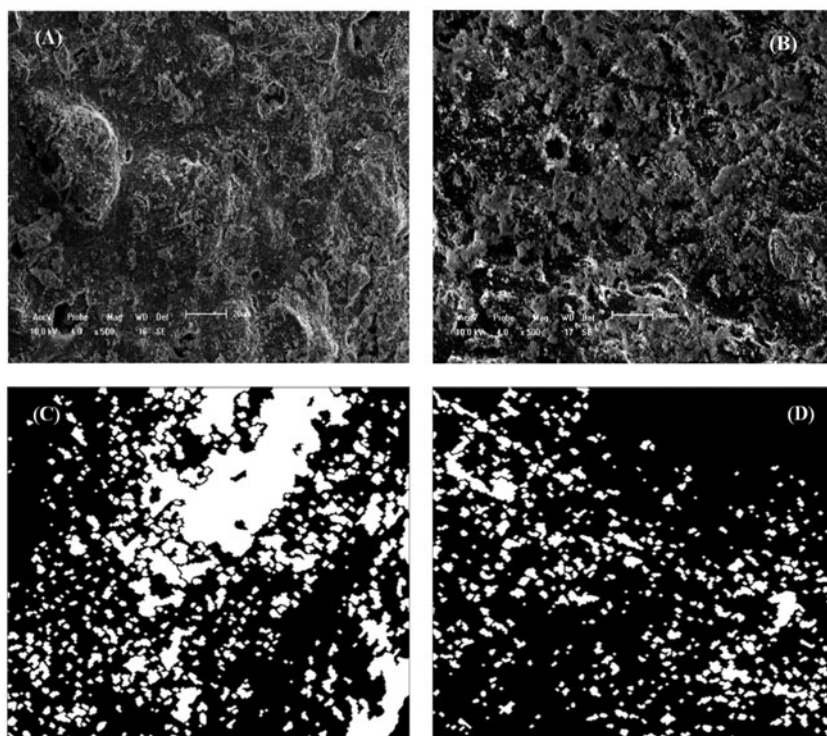


Fig. 3. SEM images of (A) the pristine Al-GCM; (B) the used Al-GCM from the adsorption column; (C) the binary diagrams of the pristine Al-GCM; and (D) the used Al-GCM from the adsorption column calculated by PCAS.

is harmful to humans, so the aluminum concentrations in the effluent were measured. The aluminum concentrations in the effluent ranged from 0.04 to 0.10 mg/L, and were lower than the Chinese drinking water quality standard (GB5749-2006), which is 0.2 mg/L [33]. We concluded, therefore, that treating wastewater containing phosphate using the Al/Ca-GCM would have little negative effect on water quality.

3.2. Taguchi analysis

A Taguchi L_9 orthogonal array method was used to optimize the conditions for removing phosphorus from water (Table 3). To evaluate the effect of each parameter on the optimization results, the acquired data BV were analyzed by applying the ANOVA method to the signal-to-noise ratios (SN_L s), using Minitab software (version 14; Minitab Inc., version 14, USA).

The nine breakthrough curves that were obtained under the specified conditions are shown in Fig. 4, and the breakthrough time and BV for each column is shown in Table 4. The shapes of the breakthrough curves indicated that phosphorus was removed from the water efficiently. Phosphorus was not detected in the effluents for the first 24 h of the tests, which sug-

Table 3
Taguchi L_9 orthogonal array method

Experiment No.	A Flow ($\mu\text{L}/\text{min}$)	B Concentration (mg/L)	C Adsorbent material
1	600	20	Ca-GCM
2	600	30	Al-GCM
3	600	40	Ca/Al-GCM
4	800	30	Ca-GCM
5	800	40	Al-GCM
6	800	20	Ca/Al-GCM
7	1,000	40	Ca-GCM
8	1,000	20	Al-GCM
9	1,000	30	Ca/Al-GCM

gests that all of the phosphorus in the water was adsorbed by the adsorbent close to the bottom of each column. The phosphorus concentration in the effluent increased gradually. Column No. 5 ($q = 800 \mu\text{L}/\text{min}$; $C_0 = 40 \text{ mg}/\text{L}$; adsorbent material = Al-GCM) reached the breakthrough point ($C_t/C_0 = 0.05$) at 52 h, indicating that the adsorbent in the lower part of the column had become saturated with solutes. The phosphorus concentration in the effluent continued to increase until it approached the concentration in the inflow

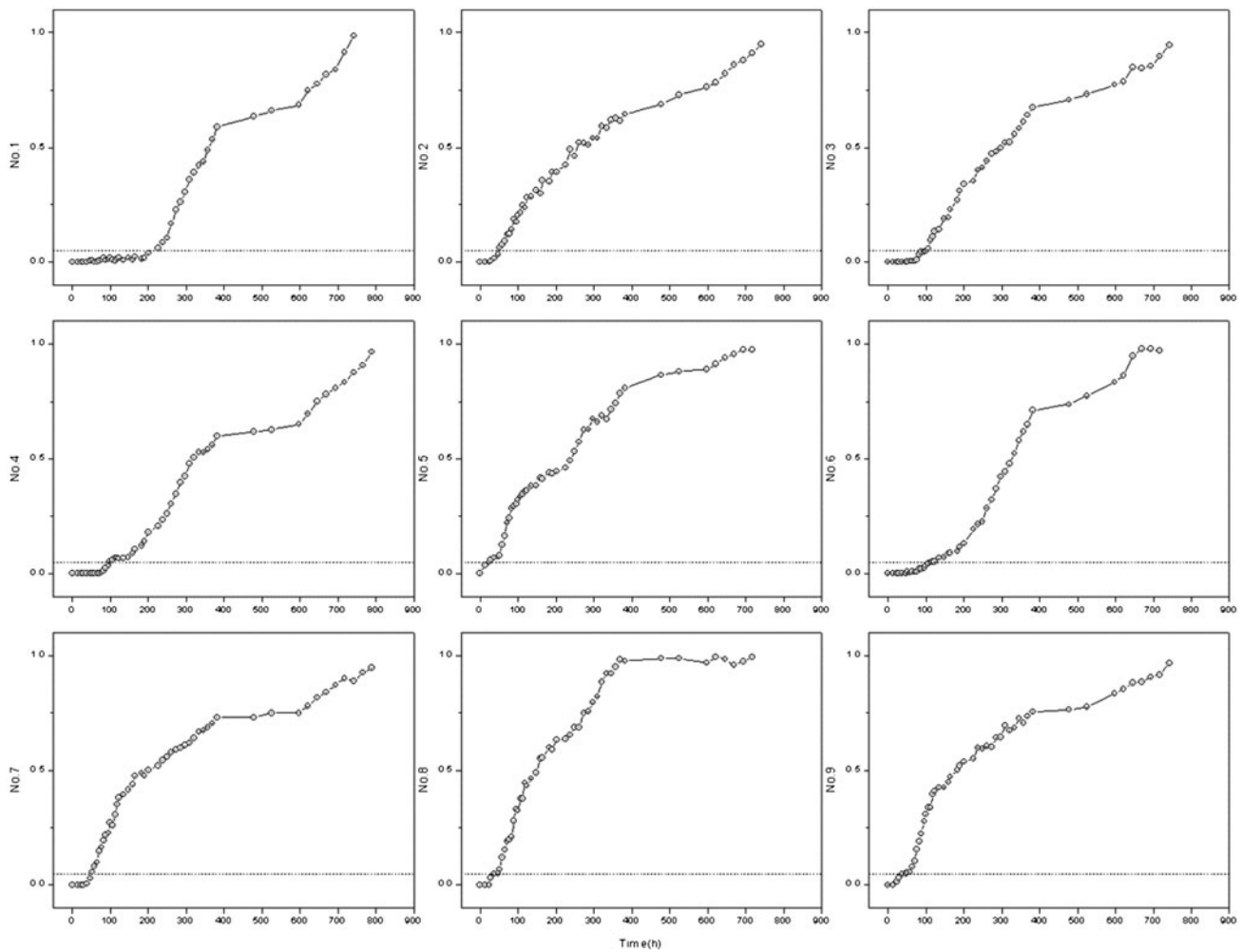


Fig. 4. Breakthrough curves of P adsorption on fixed bed for nine different conditions. The error range was all in the range of 4%, No. 1: $q = 600 \mu\text{L}/\text{min}$; $C_0 = 20 \text{ mg}/\text{L}$; Adsorbent material = Ca-GCM, No. 2: $q = 600 \mu\text{L}/\text{min}$; $C_0 = 30 \text{ mg}/\text{L}$; Adsorbent material = Al-GCM, No. 3: $q = 600 \mu\text{L}/\text{min}$; $C_0 = 40 \text{ mg}/\text{L}$; Adsorbent material = Ca-GCM & Al-GCM, No. 4: $q = 800 \mu\text{L}/\text{min}$; $C_0 = 30 \text{ mg}/\text{L}$; Adsorbent material = Ca-GCM, No. 5: $q = 800 \mu\text{L}/\text{min}$; $C_0 = 40 \text{ mg}/\text{L}$; Adsorbent material = Al-GCM, No. 6: $q = 800 \mu\text{L}/\text{min}$; $C_0 = 20 \text{ mg}/\text{L}$; Adsorbent material = Ca-GCM & Al-GCM, No. 7: $q = 1,000 \mu\text{L}/\text{min}$; $C_0 = 40 \text{ mg}/\text{L}$; Adsorbent material = Ca-GCM, No. 8: $q = 1,000 \mu\text{L}/\text{min}$; $C_0 = 20 \text{ mg}/\text{L}$; Adsorbent material = Al-GCM, No. 9: $q = 1,000 \mu\text{L}/\text{min}$; $C_0 = 30 \text{ mg}/\text{L}$; Adsorbent material = Ca-GCM & Al-GCM.

Table 4
The breakthrough time and corresponding BVs of each adsorption column

Experiment No.	1	2	3	4	5	6	7	8	9
Breakthrough point (h)	223	59	102	94	24	115	45	43	48
Bed volumes at breakthrough point	354	93	162	199	52	243	119	114	127
(Bed volumes at breakthrough point) · (C_0)	7,080	2,790	6,480	5,970	2,080	4,860	4,760	2,280	3,810

Notes: The error range was all in the range of 4%, No. 1: $q = 600 \mu\text{L}/\text{min}$; $C_0 = 20 \text{ mg}/\text{L}$; Adsorbent material = Ca-GCM, No. 2: $q = 600 \mu\text{L}/\text{min}$; $C_0 = 30 \text{ mg}/\text{L}$; Adsorbent material = Al-GCM, No. 3: $q = 600 \mu\text{L}/\text{min}$; $C_0 = 40 \text{ mg}/\text{L}$; Adsorbent material = Ca/Al-GCM, No. 4: $q = 800 \mu\text{L}/\text{min}$; $C_0 = 30 \text{ mg}/\text{L}$; Adsorbent material = Ca-GCM, No. 5: $q = 800 \mu\text{L}/\text{min}$; $C_0 = 40 \text{ mg}/\text{L}$; Adsorbent material = Al-GCM, No. 6: $q = 800 \mu\text{L}/\text{min}$; $C_0 = 20 \text{ mg}/\text{L}$; Adsorbent material = Ca/Al-GCM, No. 7: $q = 1,000 \mu\text{L}/\text{min}$; $C_0 = 40 \text{ mg}/\text{L}$; Adsorbent material = Ca-GCM, No. 8: $q = 1,000 \mu\text{L}/\text{min}$; $C_0 = 20 \text{ mg}/\text{L}$; Adsorbent material = Al-GCM, No. 9: $q = 1,000 \mu\text{L}/\text{min}$; $C_0 = 30 \text{ mg}/\text{L}$; Adsorbent material = Ca/Al-GCM.

water, at which time the entire column was saturated. Column No. 1 ($q = 600 \mu\text{L}/\text{min}$; $C_0 = 20 \text{ mg}/\text{L}$; adsorbent material = Ca-GCM) performed better than the other columns, reaching the 5% breakthrough point at 223 h. The saturation capacity of column No. 1 was $9.12 \text{ mg}/\text{g}$ (calculated from the phosphorus concentrations in the influent and effluent). In the batch studies we performed previously, the amounts of phosphorus adsorbed by the Ca-GCM increased from 1.98 to $9.51 \text{ mg}/\text{g}$ as the initial phosphorus concentration was increased from 10 to $50 \text{ mg}/\text{L}$ [22]. The higher adsorption capacity achieved in the fixed bed system could have been caused by the longer contact time between the solute and the adsorbent and by the conditions being better for the solutes to diffuse around the material. Similar results were reported by Bang et al. [34].

We used the SN_L parameter to interpret the Taguchi design results and determine the optimum conditions for the adsorption of phosphorus. The grades used to classify the influences of the test parameters on the performance statistics are given in Fig. 5. The objective of the experiment was to maximize the BV. The optimum conditions were identified using the following equation:

$$\text{SN}_L = -10 \log \left(\frac{1}{n} \sum_{i=1}^n \frac{1}{y_i^2} \right) \quad (7)$$

where SN_L is the S/N ratio, n is the number of experiments, y_i is the response of each trial using a specified combination of control factor levels, and SN_L is the ratio of the mean response to the standard deviation. A higher SN_L value indicates better system performance.

As is shown in Fig. 5(A), increasing the flow rate decreased the SN_L . Increasing the contact time may have allowed the phosphorus to penetrate the pores of the adsorbents more effectively. As is shown in Fig. 5(B), increasing the initial phosphorus concentration decreased the SN_L , the binding sites on the adsorbent in the fixed bed becoming saturated more rapidly. The breakthrough point occurred later when lower initial phosphorus concentrations were used because of the non-linearity of the adsorption process. The q/C_0 (the ratio between the amount of phosphorus adsorbed (mg/g) and the initial phosphorus concentration) value could be higher at a lower initial phosphorus concentration than at a higher concentration [35]. As is shown in Fig. 5(C), the BV of the phosphorus adsorption bed for the three kinds of adsorbent materials decreased in the order $\text{Ca-GCM} > \text{Ca}/\text{Al-GCM} > \text{Al-GCM}$, indicating that Ca-GCM was the most suitable material for the fixed bed system. In our previous batch tests, the adsorption of phosphorus by Al-GCM reached equilibrium at 12 and 24 h when the initial phosphorus concentration was 20 and $50 \text{ mg}/\text{L}$, respectively [23]. Equilibrium was reached more quickly using Ca-GCM than using Al-GCM (2.5 and 6 h, respectively) in the batch tests [22,36]. Overall, the best parameters found in the fixed bed tests described here, defined as the parameters giving the highest SN_L , were $q = 600 \mu\text{L}/\text{min}$, $C_0 = 20 \text{ mg}/\text{L}$, and material = Ca-GCM.

After the optimization study was completed, a confirmation test was performed using the optimum value that had been found for each parameter. The predicted BV (calculated at the 95% confidence interval) was 339, which was 4% lower than the actual experimental result (354).

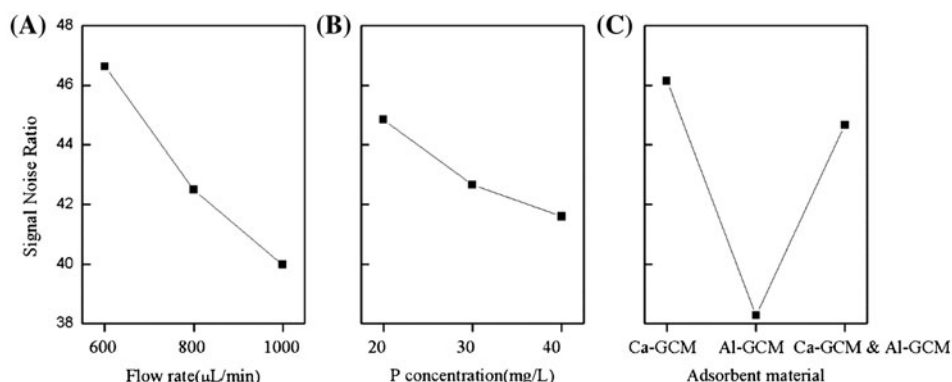


Fig. 5. The effect of flow rate (A), initial phosphorus concentration (B), and adsorbent material (C) on the SN_L in the removal of phosphorus.

As is shown in Table 5, the ANOVA gave an R^2 value of 98.53% for phosphorus removal, which indicated that the model explained 98.53% of the variability in the Taguchi method. The adjusted R^2 for the model was 94.11%, which was very similar to the actual R^2 value, indicating that there were almost no non-significant terms in the empirical model of phosphorus removal. As is shown in Table 5, the most important factor that influenced the system performance was the adsorbent material (Factor C), which was found to contribute 55.5% of the SN_L . The initial phosphorus concentration (Factor B) was the second most important factor that affected the system performance, and it was found to contribute 35.7% of the SN_L . The flow rate was found to be a relatively minor factor, contributing only 8.78% of the SN_L . The weak response of the phosphorus adsorption to the flow rate demonstrated that the adsorption process depended little on diffusion, and that the mass transfer rate could be increased at higher flow rates. These results agreed well with those reported by Guo et al. [37], although activated siderite–hematite column filters were used to remove arsenic in that study, and a weak response to the flow rate was found.

3.3. Phosphorus recycling

Recycling phosphorus from wastewater will mean that less phosphorus resources will need to be consumed, and that less phosphorus will be emitted to the aquatic environment. Therefore, phosphorus recycling is seen as an important part of the phosphorus

Table 5
ANOVA for result of experiment with SN_L as response parameter

Source	DF	SS	MS	F value	P
Flow	2	16.633	8.317	5.88	0.145
Concentration	2	67.599	33.799	23.92	0.040
Adsorbent material	2	105.010	52.505	37.15	0.026
Error	2	1,080	540	–	–
Total	8	67,037	–	–	–

Notes: The error range was 4.42%. $R^2 = 98.53\%$, R^2 (adjusted) = 94.11%, DF, degree of freedom; SS, sum of squares; MS: mean square.

removal process. The white powder that adhered to the surfaces of the adsorbents is shown in Fig. 6(A), and the results of XRD analysis of the powder are presented in Fig. 6(B). Hydroxylapatite crystals were found to be the main mineralogical component of the powder (84.79%). Li et al. [38] found similar results, and found that hydroxylapatite was formed at points of interaction between calcium and phosphate at mineral/water interfaces at pH 9.0. A small amount of augelite was also found in our end-product. Both hydroxylapatite and augelite crystals can easily be recycled because they can be used in agricultural and industrial processes. Therefore, the system described here can be used to remove phosphorus from wastewater effectively and to allow the phosphorus to be economically recycled for use in agricultural and industrial processes.

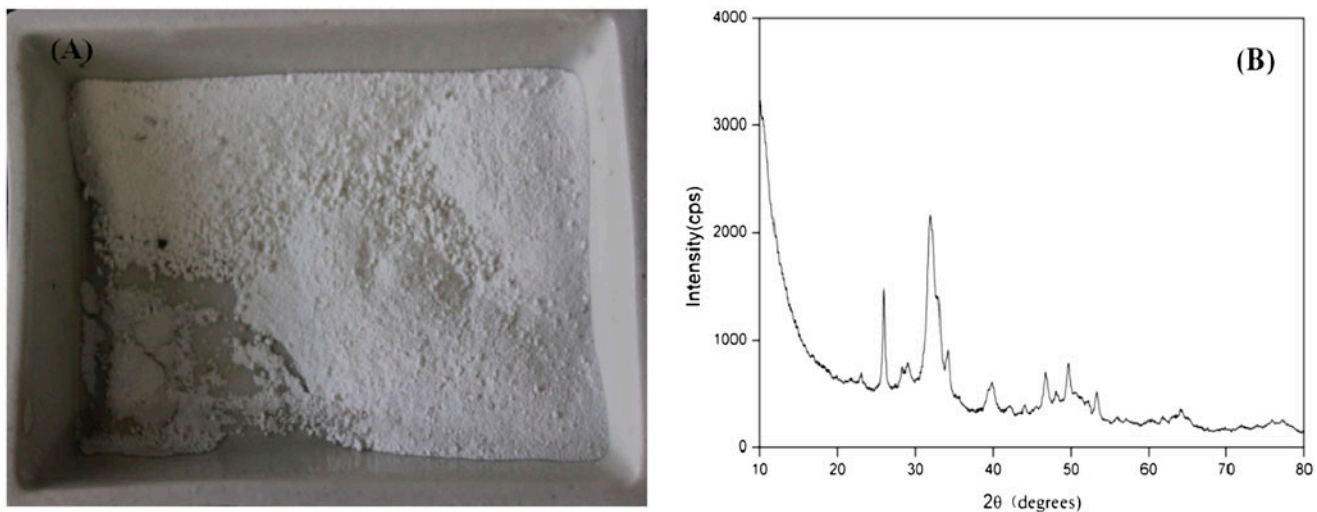


Fig. 6. Photo of white powders collected from the surface of adsorbents (A) and the XRD analysis (B).

4. Conclusions

The effects of using different adsorbent materials (Ca-GCM, Al-GCM, and Ca/Al-GCM), different initial phosphorus concentrations (20, 30, and 40 mg/L), and different flow rates (600, 800, and 1,000 $\mu\text{L}/\text{min}$) on the effectiveness of a fixed bed phosphorus removal system were investigated using the Taguchi experimental design method. The most phosphorus that was adsorbed by a material was 9.12 mg/g, and the BV was 354 under the conditions used to achieve that (material = Ca-GCM, $C_0 = 20 \text{ mg/L}$, $q = 600 \mu\text{L}/\text{min}$). The type of adsorbent material and the phosphorus concentration had the strongest effects on the phosphorus removal efficiency. It was found that phosphorus could be effectively recycled using a Ca/Al-impregnated granular clay material with a fixed bed system. The products of the adsorption process were hydroxylapatite and augelite crystals, which are good sources of phosphorus for plants and for use in other agricultural processes. Overall, our results indicate that there is strong potential for using Ca/Al-GCMs to remove phosphorus from water. However, further research will be required to identify the applications this system will be suited to and to identify new opportunities that could be exploited.

Acknowledgments

The authors thank the “Fundamental Research Funds for the Central Universities (2652013025)” and the “Beijing National Science Foundation (8144053)” for financial support for this work.

References

- [1] H.P. Weikard, D. Seyhan, Distribution of phosphorus resources between rich and poor countries: The effect of recycling, *Ecol. Econ.* 68 (2009) 1749–1755.
- [2] P.S. Lau, N.F.Y. Tam, Y.S. Wong, Wastewater nutrients (N and P) removal by carrageenan and alginate immobilized *Chlorella vulgaris*, *Environ. Technol.* 18 (1997) 945–951.
- [3] L.E. de-Bashan, Y. Bashan, Recent advances in removing phosphorus from wastewater and its future use as fertilizer (1997–2003), *Water Res.* 38 (2004) 4222–4246.
- [4] B.D. Wang, Cultural eutrophication in the Changjiang (Yangtze River) plume: History and perspective, *Estuarine Coastal Shelf Sci.* 69 (2006) 471–477.
- [5] K. Riahi, B. Ben Thayer, A. Ben Mammou, A. Ben Ammar, M.H. Jaafoura, Biosorption characteristics of phosphates from aqueous solution onto *Phoenix dactylifera* L. date palm fibers, *J. Hazard. Mater.* 170 (2009) 511–519.
- [6] K. Suzuki, Y. Tanaka, T. Osada, M. Waki, Removal of phosphate, magnesium and calcium from swine wastewater through crystallization enhanced by aeration, *Water Res.* 36 (2002) 2991–2998.
- [7] Ş. İrdemez, Y.S. Yildiz, V. Tosunoğlu, Optimization of phosphate removal from wastewater by electrocoagulation with aluminum plate electrodes, *Sep. Purif. Technol.* 52 (2006) 394–401.
- [8] T. Clark, T. Stephenson, P.A. Pearce, Phosphorus removal by chemical precipitation in a biological aerated filter, *Water Res.* 31 (1997) 2557–2563.
- [9] A.A. Randall, L.D. Benefield, W.E. Hill, Induction of phosphorus removal in an enhanced biological phosphorus removal bacterial population, *Water Res.* 31 (1997) 2869–2877.
- [10] S. Karaca, A. Gurses, M. Ejder, M. Acikyildiz, Adsorptive removal of phosphate from aqueous solutions using raw and calcinated dolomite, *J. Hazard. Mater.* 128 (2006) 273–279.
- [11] E. Oguz, Removal of phosphate from aqueous solution with blast furnace slag, *J. Hazard. Mater.* 114 (2004) 131–137.
- [12] S. Yang, Y. Zhao, R. Chen, C. Feng, Z. Zhang, Z. Lei, Y. Yang, A novel tablet porous material developed as adsorbent for phosphate removal and recycling, *J. Colloid Interface Sci.* 396 (2013) 197–204.
- [13] L. Zeng, X.M. Li, J.D. Liu, Adsorptive removal of phosphate from aqueous solutions using iron oxide tailings, *Water Res.* 38 (2004) 1318–1326.
- [14] S. Aber, A. Khataee, M. Sheydaei, Optimization of activated carbon fiber preparation from Kenaf using K_2HPO_4 as chemical activator for adsorption of phenolic compounds, *Bioresour. Technol.* 100 (2009) 6586–6591.
- [15] V.C. Srivastava, I.D. Mall, I.M. Mishra, Multicomponent adsorption study of metal ions onto bagasse fly ash using Taguchi’s design of experimental methodology, *Ind. Eng. Chem. Res.* 46 (2007) 5697–5706.
- [16] Z. Ioannou, A. Dimirkou, A. Ioannou, Phosphate adsorption from aqueous solutions onto goethite, bentonite, and bentonite-goethite system, *Water Air Soil Poll.* 224 (2013) 1374–1388.
- [17] S. Benyoucef, M. Amrani, Adsorptive removal of phosphate from aqueous solution by chemically modified biosorbent, *Desalin. Water Treat.* 44 (2012) 306–313.
- [18] W.T. Chen, C.W. Lin, P.K. Shih, W.L. Chang, Adsorption of phosphate into waste oyster shell: Thermodynamic parameters and reaction kinetics, *Desalin. Water Treat.* 47 (2012) 86–95.
- [19] C.Y. Nian, W.H. Yang, Y.S. Tarn, Optimization of turning operations with multiple performance characteristics, *J. Mater. Process. Technol.* 95 (1999) 90–96.
- [20] A.B. Engin, Ö. Özdemir, M. Turan, A.Z. Turan, Color removal from textile dyebath effluents in a zeolite fixed bed reactor: Determination of optimum process conditions using Taguchi method, *J. Hazard. Mater.* 159 (2008) 348–353.
- [21] Ş. İrdemez, Y.S. Yildiz, V. Tosunoğlu, Optimization of phosphate removal from wastewater by electrocoagulation with aluminum plate electrodes, *Sep. Purif. Technol.* 52 (2006) 394–401.
- [22] N. Chen, W. Hu, C. Feng, Z. Zhang, Removal of phosphorus from water using scallop shell synthesized ceramic biomaterials, *Environ. Earth Sci.* 71 (2013) 2133–2142.

- [23] Y. Gao, N. Chen, W.W. Hu, C.P. Feng, B.G. Zhang, Q. Ning, B. Xu, Phosphate removal from aqueous solution by an effective clay composite material, *J. Solution Chem.* 42 (2013) 691–704.
- [24] R.K. Roy, Design of experiments using the Taguchi approach: 16 steps to product and process improvement, *Technometrics* 44 (2002) 289–289.
- [25] H.S. Sii, T. Ruxton, J. Wang, Taguchi concepts and their applications in marine and offshore safety studies, *J. Eng. Design.* 12 (2001) 331–358.
- [26] A.B. Engin, Ö. Özdemir, M. Turan, A.Z. Turan, Color removal from textile dyebath effluents in a zeolite fixed bed reactor: Determination of optimum process conditions using Taguchi method, *J. Hazard. Mater.* 159 (2008) 348–353.
- [27] M. Çopur, C. Özmetin, E. Özmetin, M.M. Kocakerim, Optimization study of the leaching of roasted zinc sulphide concentrate with sulphuric acid solutions, *Chem. Eng. Process.* 43 (2004) 1007–1014.
- [28] M.R. Awual, A. Jyo, T. Ihara, N. Seko, M. Tamada, K.T. Lim, Enhanced trace phosphate removal from water by zirconium(IV) loaded fibrous adsorbent, *Water Res.* 45 (2011) 4592–4600.
- [29] N. Chen, Z. Zhang, C. Feng, M. Li, R. Chen, N. Sugiura, Investigations on the batch and fixed-bed column performance of fluoride adsorption by Kanuma mud, *Desalination* 268 (2011) 76–82.
- [30] C. Liu, B. Shi, J. Zhou, C. Tang, Quantification and characterization of microporosity by image processing, geometric measurement and statistical methods: Application on SEM images of clay materials, *Appl. Clay Sci.* 54 (2011) 97–106.
- [31] J. Ma, L. Zhu, Simultaneous sorption of phosphate and phenanthrene to inorgano-organo-bentonite from water, *J. Hazard. Mater.* 136 (2006) 982–988.
- [32] Y. Xue, H. Hou, S. Zhu, Characteristics and mechanisms of phosphate adsorption onto basic oxygen furnace slag, *J. Hazard. Mater.* 162 (2009) 973–980.
- [33] Ministry of Health of PR China, Standard for Drinking Water Quality GB5749-2006, 2006.
- [34] S. Bang, M. Patel, L. Lippincott, X.G. Meng, Removal of arsenic from groundwater by granular titanium dioxide adsorbent, *Chemosphere* 60 (2005) 389–397.
- [35] S. Ayoob, A. Gupta, P. Bhakat, Analysis of breakthrough developments and modeling of fixed bed adsorption system for As(V) removal from water by modified calcined bauxite (MCB), *Sep. Purif. Technol.* 52 (2007) 430–438.
- [36] T.E. Köse, B. Kıvanç, Adsorption of phosphate from aqueous solutions using calcined waste eggshell, *Chem. Eng. J.* 178 (2011) 34–39.
- [37] H. Guo, D. Stüben, Z. Berner, U. Kramar, Adsorption of arsenic species from water using activated siderite-hematite column filters, *J. Hazard Mater.* 151 (2008) 628–635.
- [38] W. Li, W.Q. Xu, J.B. Parise, B.L. Phillips, Formation of hydroxylapatite from co-sorption of phosphate and calcium by boehmite, *Geochim. Cosmochim. Acta* 85 (2012) 289–301.